Mathematical models of retinitis pigmentosa: The oxygen toxicity hypothesis

Roberts, Paul; Gaffney, Eamonn; Luthert, Philip; Foss, Alexander; Byrne, Helen

DOI:
10.1016/j.jtbi.2017.05.006

Document Version
Peer reviewed version

Citation for published version (Harvard):
Roberts, P, Gaffney, E, Luthert, P, Foss, A & Byrne, H 2017, 'Mathematical models of retinitis pigmentosa: The oxygen toxicity hypothesis', *Journal of Theoretical Biology*, vol. 425, pp. 53-71.
https://doi.org/10.1016/j.jtbi.2017.05.006

Mathematical Models of Retinitis Pigmentosa: The Oxygen Toxicity Hypothesis
Journal of Theoretical Biology
Supplementary Material

Paul A. Roberts*[1,2], Eamonn A. Gaffney[3], Philip J. Luthert[4], Alexander J. E. Foss[5] and Helen M. Byrne[3]

[1]Mathematical Institute, University of Oxford, Andrew Wiles Building, Radcliffe Observatory Quarter, Woodstock Road, Oxford, OX2 6GG, UK
[2]Department of Computer Science, University of Oxford, Wolfson Building, Parks Road, Oxford, OX1 3QD, UK
[3]Wolfson Centre for Mathematical Biology, Mathematical Institute, University of Oxford, Andrew Wiles Building, Radcliffe Observatory Quarter, Woodstock Road, Oxford, OX2 6GG, UK
[4]Institute of Ophthalmology, University College London, 11-43 Bath Street, London, EC1V 9EL, UK
[5]Queen's Medical Centre, Department of Ophthalmology, Derby Road, Nottingham, Nottinghamshire, NG7 2UH, UK

S1 Estimation of Parameters

Tables S1 and S2 list the dimensional parameter values used in equations (1)–(7).

S1.1 Eccentricity of the ora serrata, Θ

We fixed the boundary, Θ, to the most eccentric point reached by both the rods and cones along the temporal horizontal meridian (data provided by Curcio and published in Curcio et al., 1990).

S1.2 Oxygen diffusion coefficient, D

We take the oxygen diffusion coefficient in retinal tissue, D, to be 1.97×10^{-9} m^{2}s^{-1}, as measured by Roh et al. (1990) in the living cat at a temperature of 37–38°C.

S1.3 Retinal radius, R

The average radius of the human eye, R, is 1.2×10^{-2} m (Oyster, 1999).

*Corresponding author
E-mail address: p.a.roberts@univ.oxon.org (Paul A. Roberts)
Present address: School of Mathematics, University of Birmingham, Edgbaston Campus, Birmingham, B15 2TT, UK

S1.4 Ratio of unit surface area to unit volume, α, and healthy capillary surface area per unit volume, $\tilde{h}$

The ratio of unit surface area to unit volume, α, was calculated by taking the ratio of the surface area of the outer surface of the retinal pigment epithelium (RPE) with the volume of the retina between the outer surface of the RPE and the inner boundary of the photoreceptor inner segments (ISs) (a depth of 50μm, see Yu et al., 1994, and Webvision, `http://webvision.med.utah.edu/`). Since the inner surface of the choriocapillaris (CC) has a lobular structure, forming a continuous surface, we assume that its surface area is equal to that of the outer surface of the RPE. Therefore, we fix the healthy capillary surface area per unit volume such that $\tilde{h} = \alpha$, which corresponds to a fully vascularised CC.

S1.5 Maximum rate of oxygen uptake per photoreceptor-containing tissue unit, Q, and capillary permeability, β

The maximum rate of oxygen uptake, Q, is a combination of the oxygen uptake of an average photoreceptor (rod or cone) IS and outer segment (OS), combined with the portion of the RPE lying directly outward from it (we refer to this as a 'tissue unit'). We assume that the photoreceptors are under light adaptation (LA), since it is under these conditions, when the rate of oxygen uptake of the ISs is half that under dark adaptation (DA), that the retina will be most vulnerable to hyperoxia. We take the height of the RPE to be 5 μm and that of the ISs and OSs to be 22.5 μm each (see Yu et al., 1994, and Webvision, `http://webvision.med.utah.edu/`), whilst the area per tissue unit is assumed to be $1/\tilde{p}_A$, where $\tilde{p}_A$ is the mean photoreceptor density. The rate of oxygen uptake by the RPE is 3.00×10^{-5} Ms^{-1}, whilst that of the ISs under LA is 6.67×10^{-5} Ms^{-1} and the OSs do not consume oxygen (Birol et al., 2007; Cringle and Yu, 2002; Haugh et al., 1990; Wangsa-Wirawan and Linsenmeier, 2003). Multiplying the rate of oxygen uptake of the RPE, OSs and ISs (per unit volume) by their respective volumes (per tissue unit) and taking their sum, we obtain the maximum rate of oxygen uptake per photoreceptor-containing tissue unit:

$$\begin{aligned} Q = &(\text{rate of oxygen uptake per unit volume of RPE}) \times (\text{RPE volume per tissue unit}) \\ &+ (\text{rate of oxygen uptake per unit volume of photoreceptor OS}) \times (\text{photoreceptor OS volume per tissue unit}) \\ &+ (\text{rate of oxygen uptake per unit volume of photoreceptor IS}) \times (\text{photoreceptor IS volume per tissue unit}). \end{aligned}$$

When multiplied by the photoreceptor density (with units of photoreceptors per unit area, or, equivalently, tissue units per unit area), p, this gives the maximum rate of oxygen uptake per unit area (mol s^{-1} m^{-2}), so that upon multiplying by α, we obtain the maximum rate of oxygen uptake per unit volume (mol s^{-1} m^{-3}). We note that, by incorporating the oxygen uptake of the RPE into Q, we are assuming that the oxygen demand of the RPE is proportional to the photoreceptor density. This is reasonable, given that the RPE uses oxygen to phagocytose shed OS tips and given that it degenerates around the same time as photoreceptors are lost.

We assume that the rate of oxygen uptake by a rod is equal to that of a cone. Hoang et al. (2002) have measured the mitochondrial densities of rods and cones at a range of eccentricities in macaque and human retinas. It was found that, on average, cones contain 9-10 times more mitochondria than rods. This might lead one to expect that the rate of metabolism is greater in cones than in rods. However, the energy requirements of rods and cones are similar and the additional cone mitochondria most likely serve to enhance the cone light-gathering properties (Hoang et al., 2002). Another possibility is that cone mitochondria are less efficient than those in rods (Hoang et al., 2002). In either case, and in the absence of further information, it is reasonable to assume that the rate of oxygen uptake of a rod is the same as that of a cone. In addition, cone diameter is at its minimum in the fovea (Hoang et al., 2002), where cone density is highest, so that the disparity in the width of the ellipsoidal mitochondria containing region (and hence the number of mitochondria) between rods and cones is minimal there.

Based upon the atomic weight, charge and size of an oxygen (O_2) molecule, the capillary permeability to oxygen, β, is assumed to be of the same order of magnitude as that of sodium, which is 1.8×10^{-5} ms^{-1} (Törnquist et al., 1990).

Given that neither Q nor β are known exactly, we choose them so that the oxygen concentration across the retina, under healthy conditions, is similar in value to that found in the ISs under LA (see, for instance, Birol et al., 2007), whilst maintaining the correct order of magnitude for both parameters.

S1.6 Michaelis constant, γ

We take the Michaelis constant, γ, to equal 1 mmHg, which is within the range given by Costa et al. (1997); Goldman (2008); McGuire and Secomb (2001); Richmond et al. (1999).

S1.7 Oxygen concentration in the choriocapillaris, c_{ch}

The oxygen concentration in the CC, c_{ch}, is approximately 60 mmHg, as measured in monkeys Birol et al. (2007); Wangsa-Wirawan and Linsenmeier (2003).

S1.8 Hyperoxic threshold, c_{crit}

We choose the hyperoxic threshold, c_{crit}, to be slightly larger than the maximum steady-state oxygen concentration under healthy conditions. The qualitative behaviour of the system is not affected by our choice of c_{crit}.

S1.9 Rate of photoreceptor degeneration, δ, and intrinsic growth rate of photoreceptors, μ

The rate of photoreceptor degeneration, δ, is chosen so that degeneration occurs on a biologically realistic timescale of decades (Hartong et al., 2006). This is consistent with *in vivo* and *in vitro* measurements of the time taken for individual photoreceptors and epithelial cells to die due to hyperoxia (Sahaboglu et al., 2013; Wang et al., 2003). The intrinsic growth rate of the photoreceptors, μ, is assumed to be equal to δ, which is consistent with the timescale of photoreceptor OS regrowth (Oyster, 1999; Young, 1971).

S1.10 Rate of capillary degeneration/regrowth, η

To our knowledge, there is no quantitative data available on the rate of capillary degeneration/regrowth, η, in RP. Therefore, we consider a range of values (see Section 4.3).

S1.11 Photoreceptor profile and density parameters, B_1, B_2, B_3, b_1, b_2 b_3, and $\tilde{p}_A$

The photoreceptor profile parameters B_1, B_2, B_3, b_1, b_2 and b_3 were fitted to the mean photoreceptor profile across the temporal horizontal meridian of a sample of eight human retinas from seven individuals between 27 and 44 years in age. Data was provided by Curcio and is published in Curcio et al. (1990). Fitting was performed using Matlab's curve fitting toolbox, with the Trust-Region Reflective algorithm. This same data was used to calculate the mean healthy photoreceptor density, $\tilde{p}_A$.

S1.12 Rates of mutation-induced rod and cone degeneration, ϕ_r and ϕ_c

The rate of mutation-induced rod degeneration, ϕ_r, is introduced in non-dimensional form. We set $\phi_r = 6.6 \times 10^{-3}$, consistent with the observation that the total number of rods in the central 28.5 degrees of vision reduces by 69% between the ages of 34 and 90 (Curcio et al., 1993). In the absence of further information, we also set the rate of mutation-induced cone degeneration, $\phi_c = 6.6 \times 10^{-3}$.

S2 Mathematical Analysis of the Steady-state Problem with Capillary Degeneration

In the absence of capillary loss, this problem reduces to that of the isolated degenerate patch, considered in Section 3.2, with $\theta_2 = 1$. In this case, the stability properties of the patch are as shown in Figure 5. We anticipate that capillary loss may reduce $c(\theta_p)$, and, as a result, increase the size of the stable regions.

Table S1: Parameters associated with the dimensional model (see equations (1)–(7)). Where two sets of units are stated, the first set is consistent with the dimensional model and the second, in brackets, is that specified in the reference.

Parameter	Description	Value	Source
Θ	Eccentricity of the ora serrata	1.33 rad	Curcio et al. (1990)
D	Oxygen diffusion coefficient	1.97×10^{-9} m^{2}s^{-1}	Roh et al. (1990)
R	Retinal radius	1.2×10^{-2} m	Oyster (1999)
α	Ratio of unit surface area to unit volume of tissue	2.01×10^{4} m^{-1}	Estimated using data from Webvision and Yu et al. (1994)
Q	Maximum rate of oxygen uptake per photoreceptor containing tissue unit	1.26×10^{-17} mol s^{-1} (tissue unit)$^{-1}$	Estimated using data from Birol et al. (2007), Wangsa-Wirawan and Linsenmeier (2003)
γ	Michaelis constant	9.60×10^{-7} M (1 mmHg)	Costa et al. (1997), Goldman (2008), McGuire and Secomb (2001), Richmond et al. (1999)
β	Capillary permeability	3.6×10^{-5} m s^{-1}	Estimated using data from Törnquist et al. (1990)
$\tilde{h}$	Healthy capillary surface area per unit volume of tissue	2.01×10^{4} m^{-1}	Estimated using data from Webvision and Yu et al. (1994)
c_{ch}	Oxygen concentration in the CC	5.76×10^{-5} M (60 mmHg)	Birol et al. (2007) Wangsa-Wirawan and Linsenmeier (2003)
c_{crit}	Hyperoxic threshold	4.03×10^{-5} M	Estimate
μ	Intrinsic growth rate of photoreceptors	10^{-7} s^{-1}	Estimate
δ	Rate of photoreceptor degeneration	10^{-7} s^{-1}	Estimate
η	Rate of capillary degeneration/regrowth	10^{-11} to 10^{-6} s^{-1}	Estimate

Table S2: Parameters associated with the dimensional model (see equation (4)).

Parameter	Description	Value	Source
B_1	Cone profile parameter	1.73×10^{11} photoreceptors m^{-2}	Fitted using data from Curcio et al. (1990)
B_2	Cone profile parameter	1.76×10^{10} photoreceptors m^{-2}	Fitted using data from Curcio et al. (1990)
B_3	Rod profile parameter	8.84×10^{11} photoreceptors m^{-2}rad^{-1}	Fitted using data from Curcio et al. (1990)
b_1	Cone profile parameter	54.1 rad^{-1}	Fitted using data from Curcio et al. (1990)
b_2	Cone profile parameter	2.01 rad^{-1}	Fitted using data from Curcio et al. (1990)
b_3	Rod profile parameter	2.31 rad^{-1}	Fitted using data from Curcio et al. (1990)
$\tilde{p}_A$	Mean photoreceptor density	1.11×10^{11} photoreceptors m^{-2}	Calculated using data from Curcio et al. (1990)

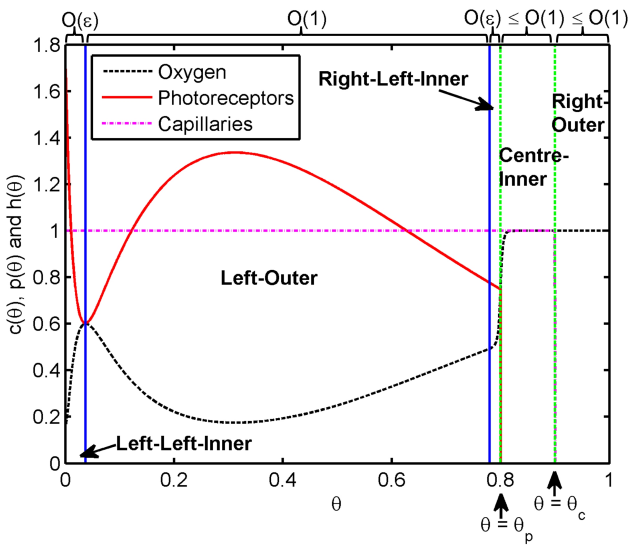

Figure S1: Diagram to show the locations of the outer and inner regions for the capillary loss analysis. The solid vertical lines demarcate the approximate limits of the boundary layers, whilst the dashed vertical lines mark the positions of θ_p and θ_c. To obtain $c(\theta)$, equations (8) and (11) were solved using the finite difference method, where $p(\theta) = H(\theta_p - \theta)\tilde{p}(\theta)$ and $h(\theta) = H(\theta_c - \theta)$. Parameter values: $\theta_p = 1.8$ and $\theta_c = 1.9$. Remaining parameter values as in Table 1.

We scale the parameters as in Section 3.2, yielding equations (21)–(23) as before (except $\beta(1-c) \mapsto \beta h(1-c)$ in equation (21)), and consider regular perturbation expansions of $c(\theta)$ and $p(\theta)$ as in equation (24), noting that $h(\theta)$ is either 1 (for $\theta \leq \theta_c$) or 0 (for $\theta > \theta_c$).

The domain may be partitioned as shown in Figure S1. The discontinuities in $p(\theta)$ at θ_p and $h(\theta)$ at θ_c divide the domain into left, centre-inner and right-outer regions and produce discontinuities in equation (21). As before, we impose continuity in the concentration and flux of oxygen at these boundaries (Bender and Orszag, 1999). The left region is further subdivided into left-left-inner, left-outer and right-left-inner regions, to allow us to satisfy the boundary conditions at $\theta = 0$ and $\theta = \theta_p$.

In the left-outer region, $p(\theta) = \tilde{p}(\theta)$ and $h(\theta) = 1$, so that equation (22) supplies $p_0(\theta) = K(\theta)$, where $K(\theta) := B_2 e^{-b_2\theta} + B_3\theta e^{-b_3\theta}$ as in Section 3.2, whilst equation (21) yields

$$c_0(\theta) = 1 - \frac{Q}{\beta}K(\theta). \tag{S1}$$

In the right-outer region, $p(\theta) = 0$ and $h(\theta) = 0$, and the kinetic terms disappear from equation (21), leaving

$$0 = \frac{\mathrm{d}^2 c}{\mathrm{d}\theta^2} + \Theta\cot(\Theta\theta)\frac{\mathrm{d}c}{\mathrm{d}\theta}, \tag{S2}$$

at leading order. Substituting $u(\theta) = \frac{\mathrm{d}c}{\mathrm{d}\theta}$ into equation (S2) and solving using the integrating factor method, we obtain $u(\theta) = A\csc(\Theta\theta)$, where A is the constant of integration. Reversing the substitution, we may use separation of variables to obtain

$$c(\theta) = A_{12}\log\left(\tan\left(\frac{\Theta\theta}{2}\right)\right) + A_{13}, \tag{S3}$$

where the A_is in this equation, and those that follow, are constants. Imposing the zero-flux boundary condition at $\theta = 1$, we find that $A_{12} = 0$. We note that, since the outer solution, $c(\theta) = A_{13}$, satisfies this boundary condition, an inner region is not required at this boundary.

The right-left- and centre-inner solutions are the same as those in Section 3.2, up to the determination of the constants of integration (see Section 3.2 for the derivation), yielding

$$c_0(\hat{\theta}^*) = 1 - \frac{Q}{\beta}K(\theta_p) + A_{14}e^{\sqrt{\frac{\beta}{D}}\hat{\theta}^*} + A_{15}e^{-\sqrt{\frac{\beta}{D}}\hat{\theta}^*}, \tag{S4}$$

in the right-left-inner region, where $p_0(\hat{\theta}^*) = K(\theta_p)$, $h(\hat{\theta}^*) = 1$ and $\hat{\theta}^* = \varepsilon^{-1}(\theta - \theta_p)$, and

$$c_0(\hat{\theta}^*) = 1 + A_{16}e^{\sqrt{\frac{\beta}{D}}\hat{\theta}^*} + A_{17}e^{-\sqrt{\frac{\beta}{D}}\hat{\theta}^*}, \tag{S5}$$

in the centre-inner region, where $p_0(\hat{\theta}^*) = 0$ and $h(\hat{\theta}^*) = 1$. (We shall not derive the left-left-inner solution, since this is not required in order to find an expression for the oxygen concentration at $\theta = \theta_p$.)

As in Section 3.2, we use Van Dyke's rule to match the left-outer and right-left-inner solutions, yielding $A_{15} = 0$. The remaining constants (A_{13}, A_{14}, A_{16}, and A_{17}) are determined by imposing continuity in the concentration and flux of oxygen at $\theta = \theta_p$ and $\theta = \theta_c$. Reverting to outer variables, this yields the right-left-inner solution,

$$c_0(\theta) = 1 - \frac{Q}{2\beta}\left(2 - \left(1 - e^{-2\varepsilon^{-1}\sqrt{\frac{\beta}{D}}(\theta_c - \theta_p)}\right)e^{-\varepsilon^{-1}\sqrt{\frac{\beta}{D}}(\theta_p - \theta)}\right)K(\theta_p), \tag{S6}$$

the centre-inner solution,

$$c_0(\theta) = 1 - \frac{Q}{2\beta}\left(e^{-2\varepsilon^{-1}\sqrt{\frac{\beta}{D}}(\theta_c - \theta_p)}e^{\varepsilon^{-1}\sqrt{\frac{\beta}{D}}(\theta - \theta_p)} + e^{-\varepsilon^{-1}\sqrt{\frac{\beta}{D}}(\theta - \theta_p)}\right)K(\theta_p), \tag{S7}$$

and the right-outer solution

$$c_0(\theta) = 1 - \frac{Q}{\beta}K(\theta_p)e^{-\varepsilon^{-1}\sqrt{\frac{\beta}{D}}(\theta_c - \theta_p)}. \tag{S8}$$

References

Bender, C. M., Orszag, S. A., 1999. Advanced Mathematical Methods for Scientists and Engineers I: Asymptotic Methods and Perturbation Theory. Springer.

Birol, G., Wang, S., Budzynski, E., Wangsa-Wirawan, N. D., Linsenmeier, R. A., 2007. Oxygen distribution and consumption in the macaque retina. Am. J. Physiol. Heart Circ. Physiol. 293 (3), H1696–H1704.

Costa, L. E., Mendez, G., Boveris, A., 1997. Oxygen dependence of mitochondrial function measured by high-resolution respirometry in long-term hypoxic rats. Am. J. Physiol. 273 (3), C852–C858.

Cringle, S. J., Yu, D. Y., 2002. A multi-layer model of retinal oxygen supply and consumption helps explain the muted rise in inner retinal PO(2) during systemic hyperoxia. Comp. Biochem. Physiol. 132 (1), 61–66.

Curcio, C. A., Millican, C. L., Allen, K. A., Kalina, R. E., 1993. Aging of the human photoreceptor mosaic: evidence for selective vulnerability of rods in central retina. Invest. Ophthalmol. Vis. Sci. 34 (12), 3278–3296.

Curcio, C. A., Sloan, K. R., Kalina, R. E., Hendrickson, A. E., 1990. Human photoreceptor topography. J. Comp. Neurol. 292 (4), 497–523.

Goldman, D., 2008. Theoretical models of microvascular oxygen transport to tissue. Microcirculation 15 (8), 795–811.

Hartong, D. T., Berson, E. L., Dryja, T. P., 2006. Retinitis pigmentosa. Lancet 368 (9549), 1795–1809.

Haugh, L., Linsenmeier, R., Goldstick, T., 1990. Mathematical models of the spatial distribution of retinal oxygen tension and consumption, including changes upon illumination. Ann. Biomed. Eng. 18, 19–36.

Hoang, Q. V., Linsenmeier, R. A., Chung, C. K., Curcio, C. A., 2002. Photoreceptor inner segments in monkey and human retina: Mitochondrial density, optics, and regional variation. Vis. Neurosci. 19 (4), 395–407.

McGuire, B. J., Secomb, T. W., 2001. A theoretical model for oxygen transport in skeletal muscle under conditions of high oxygen demand. J. Appl. Physiol. 91 (5), 2255–2265.

Oyster, C. W., 1999. The Human Eye: Structure and Function. Sinauer Associates Inc.

Richmond, K. N., Shonat, R. D., Lynch, R. M., Johnson, P. C., 1999. Critical PO(2) of skeletal muscle in vivo. Am. J. Physiol. Heart Circ. Physiol. 277 (5), H1831–H1840.

Roh, H. D., Goldstick, T. K., Linsenmeier, R. A., 1990. Spatial variation of the local tissue oxygen diffusion coefficient measured in situ in the cat retina and cornea. Adv. Exp. Med. Biol. 277, 127–136.

Sahaboglu, A., Paquet-Durand, O., Dietter, J., Dengler, K., Bernhard-Kurz, S., Ekstrom, P. A. R., Hitzmann, B., Ueffing, M., Paquet-Durand, F., 2013. Retinitis pigmentosa: rapid neurodegeneration is governed by slow cell death mechanisms. Cell Death. Dis. 4, e488.

Törnquist, P., Alm, A., Bill, A., 1990. Permeability of ocular vessels and transport across the blood-retinal-barrier. Eye 4 (2), 303–309.

Wang, X., Ryter, S. W., Dai, C., Tang, Z. L., Watkins, S. C., Yin, X. M., Song, R., Choi, A. M. K., 2003. Necrotic cell death in response to oxidant stress involves the activation of the apoptogenic Caspase-8/Bid pathway. J. Biol. Chem. 278 (31), 29184–29191.

Wangsa-Wirawan, N. D., Linsenmeier, R. A., 2003. Retinal oxygen: Fundamental and clinical aspects. Arch. Ophthalmol. 121 (4), 547–557.

Young, R. W., 1971. The renewal of rod and cone outer segments in the rhesus monkey. J. Cell Biol. 49, 303–318.

Yu, D. Y., Cringle, S. J., Alder, V. A., Su, E. N., 1994. Intraretinal oxygen distribution in rats as a function of systemic blood pressure. Am. J. Physiol. Heart. Circ. Physiol. 267 (6), H2498–H2507.